

Phase separation in $\text{La}_2\text{CuO}_{4+y}$ ceramics probed by dielectric measurements

C. C. Wang,¹ Y. M. Cui,¹ G. L. Xie,¹ C. P. Chen,² and L. W. Zhang^{1,3,*}

¹*Department of Physics, Tsinghua University, Beijing 100084, People's Republic of China*

²*Department of Physics, Peking University, Beijing 100871, People's Republic of China*

³*Laboratory of Advanced Materials, Tsinghua University, Beijing 100084, People's Republic of China*

(Received 27 January 2005; revised manuscript received 25 April 2005; published 12 August 2005)

The low-frequency (10^2 – 10^5 Hz) dielectric properties and dc resistivity of oxygen-doped $\text{La}_2\text{CuO}_{4+y}$ ceramic samples were investigated as a function of temperature (23–300 K). The as-prepared sample featuring phase separation shows very high dielectric constant $\epsilon' > 10^5$ above 150 K, which was found to originate from the hopping motion of localized holes. Below 150 K, the relaxation process due to the condensation of the holes can be observed in the dielectric spectra. When the sample was annealed at different temperatures in reduced atmosphere to tune the oxygen content, the phase separation disappears accompanied by the absence of the relaxation in the annealed sample. Our results give strong support to the phase separation model and evidence the inhomogeneous distribution of holes in the oxygen-doped $\text{La}_2\text{CuO}_{4+y}$ ceramic samples investigated.

DOI: [10.1103/PhysRevB.72.064513](https://doi.org/10.1103/PhysRevB.72.064513)

PACS number(s): 74.72.Dn, 77.22.Gm

I. INTRODUCTION

One of the most interesting and intensively investigated issues in the field of high-temperature superconductivity is the possibility that the cuprates possess an inherent inhomogeneous distribution of charge carriers in the electronically active CuO_2 planes. Several theoretical models, for example, the two-component model^{1,2} and the ferronic model,^{3,4} have predicted that the polarized clusters induced by holes in CuO_2 planes have the tendency to come close to each other at low enough temperatures, resulting in an electric inhomogeneity in cuprates. Charge inhomogeneities, in terms of phase separation or stripe phase have been hinted by various techniques, such as Mössbauer spectroscopy,⁵ photodoping experiments,⁶ neutron scattering experiments,⁷ electron paramagnetic resonance experiments,⁸ and so on.

Phase separation results in the formation of metallic hole-rich microdomains and insulating hole-poor regions. In this scenario, it is natural to expect different physical meanings of the dynamical response, since an external electric field, inducing an electric current along the material (due to hopping of the holes), produces a charge carrier concentration discontinuity across the domain walls. The charge buildup would lead to a Debye-like behavior of Maxwell-Wagner relaxation. Hence, knowledge from the dielectric properties would provide some meaningful information about phase separation. Indeed, experiments in La_2CuO_4 single crystals have revealed some interesting results, such as high dielectric constant,^{9–11} hopping conductivity,^{12,13} and even extremely heavy charge carriers, also reported from millimeter-wave conductivity measurements.⁹ However, experimental work on dynamical properties of La_2CuO_4 ceramic samples is still scarce. A Debye-type dielectric behavior and variable-range-hopping conductivity have been reported at high frequency (9 GHz) and low temperature range (5–150 K) in ceramic La_2CuO_4 samples.¹⁴ Unfortunately, the dielectric behavior at low frequencies was not reported. Rey *et al.*¹⁵ found unexpected large dielectric constants in ceramic, non-

metallic $\text{YBa}_2\text{Cu}_3\text{O}_{3+\delta}$ in the frequency range of 20 Hz to 1 MHz. These results strongly indicate that ceramic samples also have important information compared with their counterpart single-crystal samples.

In this paper, we report our measurements of dielectric properties in oxygen-doped polycrystalline $\text{La}_2\text{CuO}_{4+y}$. $\text{La}_2\text{CuO}_{4+y}$ has been chosen because it possesses a phase separation miscibility gap^{16–18} which exhibits the coexistence of superconducting and antiferromagnetic (AF) phases, when the content of excess oxygen y is in the region $0.01 \leq y \leq 0.055$. Most of the experimental evidence for phase separation was obtained in this kind of material. We find the dielectric constants are substantially larger than all previously reported values in La-based cuprates. Our results can be well described in the framework of phase separation and evidence the inhomogeneous distribution of holes in the investigated material.

II. EXPERIMENTAL DETAILS

Ceramic $\text{La}_2\text{CuO}_{4+y}$ samples with a density of 85% of the theoretical value of 7.11 g/cm^3 were prepared by conventional solid-state reaction. Excess oxygen was inserted into the samples by the vapor-doping method.¹⁹ In brief, single-phase La_2CuO_4 pellets with CuO powder nearby were sintered at 1100°C for 20 h followed by slow cooling. In this process the CuO powder is used to achieve the oxygen atmosphere with the decomposing of CuO at $\sim 1000^\circ\text{C}$. In order to investigate the effects of the oxygen content on the dielectric properties, some as-prepared samples were annealed in flowing (200 ml/min) N_2 (with purity $>99.999\%$) with carbon powder as oxygen getter at 400 and 800°C for 2 h, denoted as steps A1 and A2, respectively. The annealing temperatures have been chosen because it was found²⁰ that interstitial oxygen effuses largely between 270 and 400°C , while lattice oxygen releases around 800°C . To study the dynamical properties, Au electrodes were sputtered on opposite sides of a $\text{La}_2\text{CuO}_{4+y}$ pellet. The low-frequency

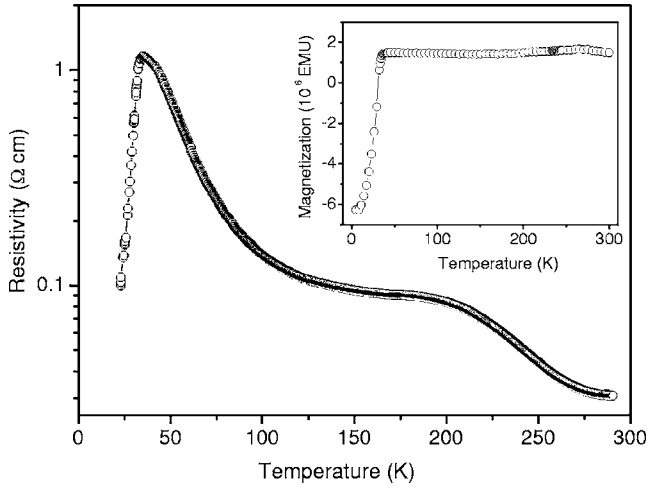


FIG. 1. Temperature dependence of the resistivity of an as-prepared $\text{La}_2\text{CuO}_{4+y}$ ceramic. Inset shows the temperature-dependent magnetization of the sample.

(<1 MHz) dielectric measurements were performed with a QuadTech 1730 LCR Digibridge in a cooling run from room temperature to ~ 23 K, followed by a heating run to room temperature. The data of both runs were reproducible and reversible. dc resistivity was measured by the four-probe technique. Magnetization measurements were carried out in the zero-field-cooled state with a Quantum Design superconducting quantum interference design (SQUID) magnetometer in a field of 50 Oe.

III. RESULTS AND DISCUSSIONS

Figure 1 shows the temperature dependence of the dc resistivity for an as-prepared $\text{La}_2\text{CuO}_{4+y}$ ceramic. It is seen that the insulator-superconductor $\text{La}_2\text{CuO}_{4+y}$ transition occurs at 35 K in agreement with previous reports²¹ for lightly doped ($y \leq 0.05$) $\text{La}_2\text{CuO}_{4+y}$ samples showing a stable superconducting phase with transition temperature $T_C \sim 32\text{--}35$ K. A noteworthy feature is that with decreasing temperature, the resistivity exhibits two increasing steps. One occurs at about 120 K followed by the superconducting transition, while the other is located at 200–250 K, which was frequently observed in the literature, but its mechanism is not clear so far. The magnetization of the as-prepared sample (inset of Fig. 1) clearly shows two phase transitions: a superconducting phase transition at $T_C \sim 35$ K and an AF phase transition at $T_N \sim 270$ K, suggesting the existence of phase separation.

The temperature dependence of the real (ϵ') and imaginary (ϵ'') parts of the complex permittivity for the as-sintered sample is presented in Fig. 2. Both ϵ' and ϵ'' have considerably large values surpassing 10^5 at high temperatures. Above ~ 120 K, the $\epsilon'(T)$ responses for all the measured frequencies are nearly exponential. However, below 120 K they show noticeable decrease. This deviation from the exponential law becomes pronounced with increasing frequency. The demarking temperature coincides with the starting of the low-temperature drastic increasing step in resistivity (Fig. 1) which is a characteristic of the condensation of the polarized

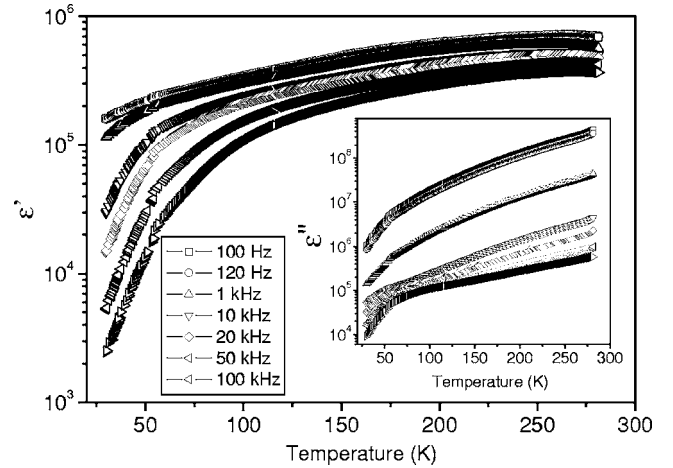


FIG. 2. The real (ϵ') and imaginary (ϵ'' , inset) parts of the permittivity at different frequencies as a function of temperature for the as-prepared ceramic $\text{La}_2\text{CuO}_{4+y}$ sample.

clusters as discussed earlier.²² This result is a strong indication of the affinity between the observed dielectric behaviors and phase separation.

At high temperatures the holes localized by polaronic clusters in the Cu-O plane can make a contribution to conductivity by hopping. Under an external ac electric field, the hopping motion gives rise to dipolar effect and sizable polarization with the in-phase and out-of-phase components responsible for the real and dielectric loss $\tan \delta$, respectively. Qualitatively, the frequency dependence of hopping conductivity can be well described by the so-called universal dielectric response²³ (UDR)

$$\sigma'(\omega) = \sigma_{dc} + \sigma_0 \omega^s, \quad (1)$$

where σ_{dc} is the dc conductivity of the sample, $\omega (=2\pi f)$ is the angular frequency, and σ_0 and the frequency exponent s are temperature-dependent constants.

Within the UDR model, ϵ' can be calculated as

$$\epsilon' = \tan(s\pi/2) \sigma_0 \omega^{s-1} / \epsilon_0, \quad (2)$$

where ϵ_0 is the electric permittivity of free space. Equation (2) can be rewritten as

$$\omega \epsilon' = A(T) \omega^s, \quad (3)$$

where the temperature-dependent constant $A(T) = \tan(s\pi/2) \sigma_0 / \epsilon_0$.

Therefore, for a given temperature, a straight line with a slope s should be obtained if $\log_{10}(\omega \epsilon')$ is plotted as a function of $\log_{10} \omega$. This inference was confirmed on the log-log graph in Fig. 3. The perfect linear relation is clearly seen at all the measured frequencies for $T > 150$ K. However, for $T < 100$ K, the experimental data deviate from the linear behavior at highest frequencies. As temperature decreases, the deviation becomes more pronounced. These results are expected based on the theory of phase separation. When the temperature decreases, the isolated polarized clusters begin to condense, leading to a decrease in the number of the cluster and the formation of microdomains. The former effect

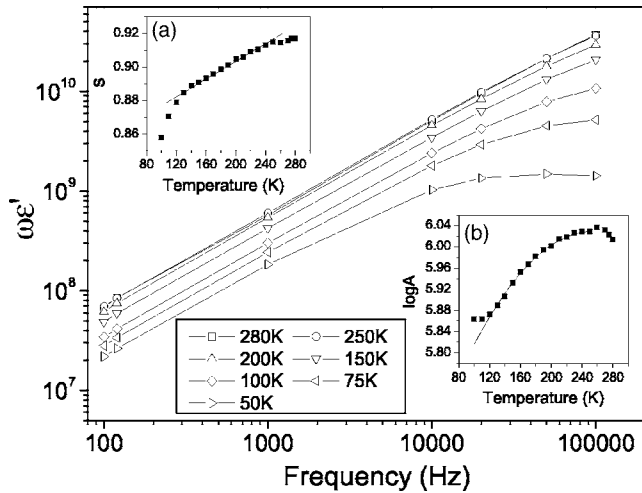


FIG. 3. Plot of $\log_{10}(\omega\epsilon')$ against $\log_{10}\omega$ at fixed temperatures for the as-prepared sample. Insets (a) and (b) show the temperature dependence of s and $\log_{10}A$ obtained from the best linear fittings based on Eq. (3). The solid curves in insets (a) and (b) are results calculated from Eqs. (4) and (5), respectively.

will lower the polarization due to the reduction of the dipolar effect at all the measured frequencies to the same extent, i.e., shift the straight line in the plot of $\log_{10}(\omega\epsilon')$ vs $\log_{10}\omega$ to low values of $\log_{10}(\omega\epsilon')$. The latter effect, however, will become inactive first in the high-frequency range due to the slow dynamics of the domain walls and result in the observed deviation from the linear behavior. Obviously, the deviation will become more and more pronounced as the domains grow in size with decreasing temperature. The above analysis also suggests that in our experiments the small polarized clusters begin to condense at the temperature range between $T=150$ and 100 K, consistent with the resistivity measurements in Fig. 1.

To obtain more information about phase separation from the dielectric behaviors, the values of s and $\log_{10}A$ at different temperatures deduced from the best linear fittings based on Eq. (3) were presented, respectively, in insets (a) and (b) of Fig. 3. It is clear that the general behavior of s and $\log_{10}A$ is to decrease with lowering of the temperature. At $T=250$ K, corresponding to the high-temperature increasing step in resistivity (Fig. 1), s exhibits a steplike increase, while $\log_{10}A$ shows a steplike decrease with decreasing temperature. In the temperature range from $T=250$ to 120 K, the data points of s can be linearly fitted with the expression

$$s = 0.8504 + 2.6493 \times 10^{-4}T, \quad (4)$$

while the behavior of $\log_{10}A$ can be described by the polynomial

$$\log_{10}A = -8.9794 \times 10^{-6}T^2 + 0.004567T + 5.4502. \quad (5)$$

The solid curves in the insets (a) and (b) of Fig. 3 are the results of the least-squares fittings according to Eqs. (4) and (5), respectively.

At $T=120$ K, corresponding to the beginning of the low-temperature increasing step in resistivity (Fig. 1), the data points of s and $\log_{10}A$ no longer obey Eqs. (4) and (5),

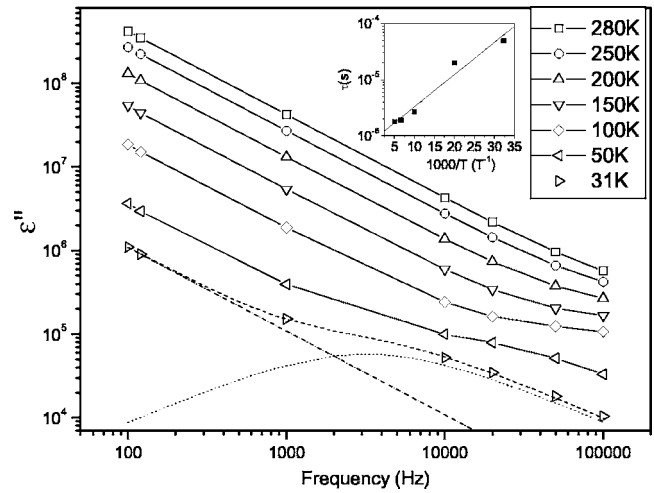


FIG. 4. $\log_{10}(\epsilon'')$ versus $\log_{10}\omega$ at fixed temperatures for the as-prepared sample. The solid curves are guides to the eye, the dash-dotted line indicates the contribution to ϵ'' from conductivity, the dotted curve is the contribution from relaxation, and the dashed curve is the total of the two contributions. The inset shows the temperature dependence of the mean relaxation time. The solid line in the inset is the fitting result to the Arrhenius law.

respectively, indicating the occurrence of a different physical process, i.e., the condensation of the polarized clusters.

Therefore, both parameters obtained from the dielectric behavior accurately describe the electrical features presented in Fig. 1 and the underlying physical process—phase separation.

We now turn to discuss the imaginary part of the complex permittivity. Figure 4 shows the log-log plot of $\epsilon''(\omega)$ versus frequency at fixed temperatures. The low-frequency data points of $\epsilon''(\omega)$ follow a straight line with a common negative slope of -1 . This feature is the hallmark that the energy dissipation labeled as $\epsilon''(\omega)$ is dominated by the conductivity. At $T=280$ K, all the experimental data fall on a straight line in the frequency range covered, indicating that only the conductivity has a contribution to $\epsilon''(\omega)$. With decreasing temperature, the data points of $\epsilon''(\omega)$ deviate from the straight line at the high-frequency limit. This deviation becomes much more evident at $T \leq 100$ K. This fact is also a substantial proof for the condensation of the polarized clusters, because, as mentioned above, with increasing size of the microdomains due to the coalescence of small clusters, the slow dynamics of the domain walls results in the delay of the response to the external alternating field, especially at high frequencies. Hence, another kind of energy dissipation mechanism arising from “relaxation” comes into action first in the high-frequency range. In fact, two different regimes can be identified in Fig. 4: a low-frequency dissipation regime related to charge transport and the relaxation regime, active to higher frequency, and originating from the relaxation of the condensed clusters. Statistically, the condensed clusters are expected to be varied in size; thereby the relaxation behavior of the domain walls is expected to be a poly-dispersive process with a distribution of relaxation time. Hence the Cole-Cole model²⁴ is adopted to evaluate the dielectric relaxation. The complex permittivity can therefore be expressed by

$$\varepsilon^* = \varepsilon_\infty + (\varepsilon_0 - \varepsilon_\infty) / [1 + (i\omega\tau)^{1-\alpha}], \quad (6)$$

where i is the imaginary unit, τ is the mean relaxation time, and α is an empirical constant with a value between 0 and 1. The case $\alpha=0$ corresponds to the Debye model that has a single relaxation time. Considering the two contributions (conductivity and relaxation) and according to Eqs. (1) and (6), $\varepsilon''(\omega)$ can be written as

$$\varepsilon'' = \sigma_{dc}/\omega + \sigma_0\omega^{\alpha-1} + (\Delta\varepsilon/2)\sin(\beta\pi/2)/[\cosh(\beta z) + \cos(\beta z)], \quad (7)$$

where $\Delta\varepsilon = \varepsilon_0 - \varepsilon_\infty$, $\beta = 1 - \alpha$ and $z = \ln(\omega\tau)$. The second term of Eq. (7) comes from the Kramers-Kronig transformation of Eq. (2) and thus can be calculated from Eqs. (4) and (5) with values found to be negligible.

By fitting the experimental data to Eq. (7), we can distinguish the two contributions to $\varepsilon''(\omega)$. As an example, the least-squares fitting to the data points at 31 K were also plotted in Fig. 4. The fitting is perfect, indicating that the model used is suitable. In addition, as shown in the inset of Fig. 4, the obtained τ follows approximately the Arrhenius law

$$\tau = \tau_0 \exp[E/(k_B T)], \quad (8)$$

where τ_0 is the relaxation time at infinite temperature, E is the activation energy for relaxation, and k_B is the Boltzmann constant. The activation energy E was found to be 8.34 meV, corresponding to a temperature value of 96.8 K, very close to the dc conductivity activation energy of 100 K found in a crystal La_2CuO_4 sample.⁹

Therefore, the present results give strong support to phase separation and evidence the inhomogeneous distribution of holes in $\text{La}_2\text{CuO}_{4+y}$. In $\text{La}_2\text{CuO}_{4+y}$, crucial to phase separation is the content of excess oxygen, which was reported to be very sensitive to thermal treatments.^{20,25} Hence, the dielectric behaviors of the sample exhibiting phase separation are expected to show strong dependence on oxygen content. To clarify this expectation, after the dielectric measurements, the as-prepared sample was subjected to two consecutive annealing steps: step A1 and step A2. After each step, the resistivity and dielectric behaviors were measured as a function of temperature. The inset of Fig. 5 shows the resistivity behavior after step A1. Compared with the results before step A1 (Fig. 1), notable changes can be seen: (1) The resistivity increases by several orders of magnitude; (2) superconductivity does not appear down to 23 K; (3) the high-temperature increasing step in resistivity disappears completely. These results imply that the excess oxygen essential to superconductivity and phase separation emits greatly during step A1.

The main panel of Fig. 5 provides the temperature dependence of ε' and ε'' of the sample after step A1. It is seen that ε' is reduced by two orders of magnitude compared with the results of the as-prepared sample (Fig. 2), confirming the large decrease of holes due to the emission of the excess oxygen. Note that ε' becomes nearly frequency and temperature independent at the lowest temperatures. This fact indicates that the observed response represents the static dielectric response of the material without the dipolar effects, thereby evidencing the absence (or great weakening) of the

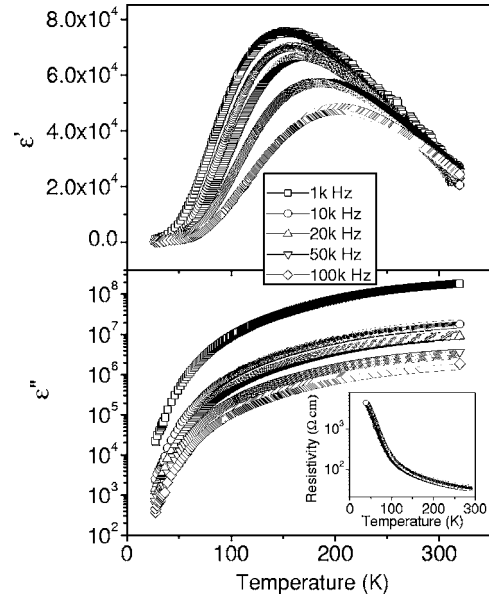


FIG. 5. Temperature-dependent ε' and ε'' at different frequencies for the sample annealed in N_2 at 400°C for 2 h. The inset shows the variation of resistivity with temperature after this annealing treatment.

hopping motion of the holes. Meanwhile, ε' exhibits a broad peak around 150 K with the peak position shifts to higher temperatures as the measured frequency increases. Similar behavior has been found in a Zn-doped La_2CuO_4 single crystal²⁶ near the Néel temperature, and was thought to suggest the possibility of an enhanced electrical polarizability by antiferromagnetic ordering. However, the peak position in our present work appears lower than the Néel temperature (>270 K); thus, further studies remain to be done to clarify this fact. The temperature dependence of ε'' has similar behavior on the whole to that before step A1 (Fig. 2). Profound changes can be seen from the frequency dependence of ε'' in the log-log plot shown in Fig. 6. It is found that the experimental data points for all the seven chosen temperatures fall nearly on straight lines with a common slope of -1 in the

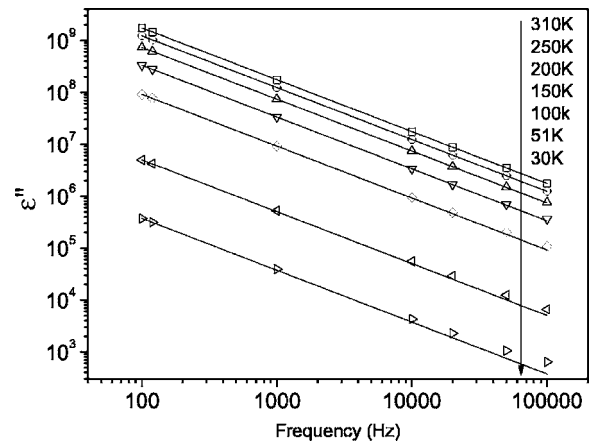


FIG. 6. Plot of $\log_{10}(\varepsilon'')$ against $\log_{10} \omega$ at fixed temperatures for the 400°C N_2 -annealed sample. The solid lines are fitting curves with a common slope of -1 .

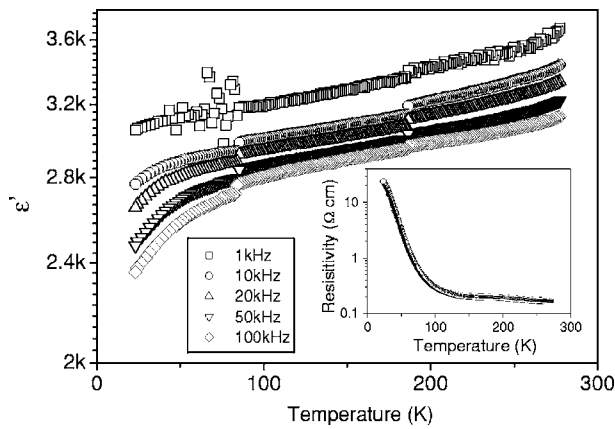


FIG. 7. Variation of ϵ' and ϵ'' with temperature at different frequencies for the sample annealed in N_2 at 800°C for 2 h. The inset shows resistivity against temperature after this annealing treatment.

frequency window. This result indicates that the conductivity has overwhelming contribution to energy dissipation, further evidencing that phase separation has been spoiled by step A1. It should be emphasized that this conductivity might be different from that caused by the hopping motion of holes and might arise from the hopping motion of the localized electron carriers due to Anderson location.²⁷

The temperature dependence of the resistivity after step A2 is plotted in the inset of Fig. 7. It is found that the treatment of step A2 makes the resistivity decrease. This is because the effusion of lattice oxygen leads to the creation of oxygen vacancies which has a contribution to the conductivity as previously reported.²⁰ It is interesting to note that the high-temperature increasing step in resistivity emerges again. This result suggests that the oxygen vacancy carriers might have similar transport behavior to that of the hole carriers. Therefore, the presence of a similar dielectric behavior of ϵ' as a function of temperature after step A2, shown in the main panel of Fig. 7, is anticipated. However, the frequency dependence of ϵ'' (see Fig. 8) shows no evident contribution from the relaxation like that after step A1, implying that no phase separation exists in the annealed sample after step A2 as well as step A1. A striking result found in the sample after step A2 is that a linear dependence of dielectric loss tangent with temperature can be observed when $T \geq 50\text{ K}$, as seen from the inset of Fig. 8. The same result has been reported in $\text{Na}_{0.88}\text{Li}_{0.12}\text{NbO}_3$ ceramics.²⁸ Obviously, the appearance of this linear dependence has a close relation with the oxygen vacancy; details about the relationship will be discussed elsewhere.

Finally, it is worth pointing out that although we cannot directly determine the exact excess oxygen doping level of all samples, the value of $T_C \sim 35\text{ K}$ and the coexistence of

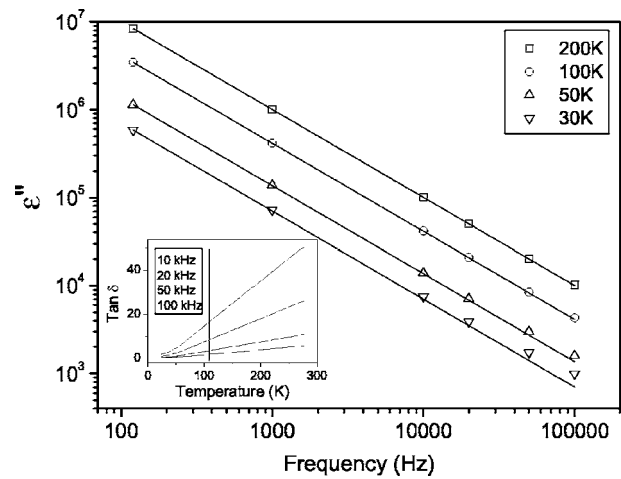


FIG. 8. Plot of $\log_{10}(\epsilon'')$ against $\log_{10} \omega$ at fixed temperatures for the 800°C N_2 -annealed sample. The inset shows the temperature dependence of the dissipation factor at different frequencies for the sample.

superconducting and antiferromagnetic transitions imply that the oxygen content of the as-prepared samples should be in the miscibility gap. Annealing in pure nitrogen with carbon powder as an oxygen getter at high temperatures (steps A1 and A2) would effectively remove the interstitial oxygen and the lattice oxygen, respectively. Therefore the qualitative conclusion could be correctly obtained by comparing the electric and dielectric properties of the as-prepared sample with the sample after steps A1 and A2.

IV. CONCLUSIONS

The low-frequency dielectric behaviors of $\text{La}_2\text{CuO}_{4+y}$ ceramics have been investigated in detail. In the as-prepared sample, the dielectric behaviors are consistent with the phase separation model and can be interpreted in terms of the hopping motion of polarized clusters created by the holes. Annealing treatments in a reducing atmosphere (nitrogen) at different temperatures destroy phase separation and the corresponding dielectric behaviors are quite different from those of the as-prepared samples. Hence, the results suggest that the investigation of dielectric properties is a valid and easy tool to characterize phase separation in high-temperature superconductors.

ACKNOWLEDGMENTS

This work was financially supported by National 973 Project of China, National Natural Science Foundation of China (Grant No. 10474050), and Tsinghua University Natural Science Foundation. We acknowledge useful discussions with Professor G. M. Zhang.

- *Corresponding author. Email address: Lwzhang@tsinghua.edu.cn
- ¹L. P. Gor'kov and A. V. Sokol, JETP Lett. **46**, 420 (1987).
- ²L. P. Gor'kov, J. Supercond. **13**, 765 (2000).
- ³V. Hizhnyakov and E. Sigmund, Mater. Lett. **9**, 425 (1990); Physica C **165**, 655 (1988).
- ⁴V. Hizhnyakov, N. N. Kristoffel, and E. Sigmund, Physica C **160**, 119 (1989); **161**, 435 (1989).
- ⁵J. A. Hodges, P. Bonville, P. Imbert, and G. Jéhanno, Physica C **184**, 259 (1991).
- ⁶G. Yu, C. H. Lee, A. J. Heeger, N. Herron, and E. M. McCarron, Phys. Rev. Lett. **67**, 2581 (1991).
- ⁷J. Mesot, P. Allenspach, U. Staub, A. Furrer, and H. Mutka, Phys. Rev. Lett. **70**, 865 (1993).
- ⁸P. G. Baranov and A. G. Badalyan, Solid State Commun. **85**, 987 (1993).
- ⁹D. Reagor, E. Ahrens, S.-W. Cheong, A. Migliori, and Z. Fisk, Phys. Rev. Lett. **62**, 2048 (1989).
- ¹⁰C. Y. Chen, N. W. Preyer, P. J. Picone, M. A. Kastner, H. P. Jenssen, D. R. Gabbe, A. Cassanho, and R. J. Birgeneau, Phys. Rev. Lett. **63**, 2307 (1989).
- ¹¹C. Y. Chen, R. J. Birgeneau, M. A. Kastner, N. W. Preyer, and T. Thio, Phys. Rev. B **43**, 392 (1991).
- ¹²P. Lunkenheimer, M. Resch, A. Loidl, and Y. Hidaka, Phys. Rev. Lett. **69**, 498 (1992).
- ¹³P. Lunkenheimer, G. Knebel, A. Pimenov, G. A. Emel'chenko, and A. Lodl, Z. Phys. B: Condens. Matter **99**, 507 (1996).
- ¹⁴J. Tateno, N. Masaki, and A. Iwase, Phys. Lett. A **138**, 313 (1989).
- ¹⁵C. M. Rey, H. Mathias, L. R. Testardi, and S. Skirius, Phys. Rev. B **45**, 10639 (1992).
- ¹⁶J. C. Grenier, N. Lagueyte, A. Wattiaux, J. P. Doumerc, P. Dordor, J. Etourneau, M. Pouchard, J. D. Goodenough, and J. S. Zhou, Physica C **202**, 209 (1992).
- ¹⁷P. G. Radaelli, J. D. Jorgensen, R. Kleb, B. A. Hunter, F. C. Chou, and D. C. Johnston, Phys. Rev. B **49**, 6239 (1994).
- ¹⁸B. O. Wells, Y. S. Lee, M. A. Kastner, R. J. Christianson, R. J. Birgeneau, K. Yamada, Y. Endoh, and G. Shirane, Science **277**, 1067 (1997).
- ¹⁹C. C. Wang, X. Zheng, and J. Zhu, Europhys. Lett. **63**, 590 (2003).
- ²⁰Y. H. Fang and P. H. Hor, Physica C **341–348**, 565 (2000).
- ²¹H. H. Feng, Z. G. Li, P. H. Hor, S. Bhavaraju, J. F. DiCarlo, and A. J. Jacobson, Phys. Rev. B **51**, 16499 (1995).
- ²²C. C. Wang and J. Zhu, Semicond. Sci. Technol. **16**, 518 (2003).
- ²³A. K. Jonscher, *Dielectric Relaxation in Solids* (Chelsea Dielectrics Press, London, 1983).
- ²⁴K. S. Cole and R. H. Cole, J. Chem. Phys. **9**, 341 (1941).
- ²⁵Z. G. Li, H. H. Feng, Z. Y. Yang, A. Hamed, S. T. Ting, P. H. Hor, S. Bhavaraju, J. F. DiCarlo, and A. J. Jacobson, Phys. Rev. Lett. **77**, 5413 (1996).
- ²⁶G. Cao, J. W. O'Reilly, J. E. Crow, and L. R. Testardi, J. Appl. Phys. **75**, 6595 (1994).
- ²⁷N. F. Mott and E. A. Davis, *Electronic Processes in Noncrystalline Materials*, 2nd ed. (Clarendon, Oxford, 1979).
- ²⁸M. A. L. Nobre and S. Lanfredi, J. Phys. Chem. Solids **62**, 1999 (2001).